Effect of grain orientation on tantalum magnetron sputtering yield

Z. Zhang, Ling Kho, and C. E. Wickersham, Jr.[a)]
Cabot Corporation, 1255 Kinnear Road, Columbus, Ohio 43212

(Received 27 March 2006; accepted 16 May 2006)

The differential sputter yields of tantalum grains during argon ion magnetron sputtering were measured and found to correlate with the atomic packing density in the uppermost atomic layer. Grains with their (110) planes aligned within 15° of the sputtering surface had the highest sputtering yield (0.95 at./ion at 400 eV). Simultaneously, grains oriented so that their (111) planes were within 15° of the sputtering surface had sputtering yields of around two times lower (0.47 at./ion at 400 eV). These results are consistent with the surface sputtering rather than the channeling model. A correlation was found between the number of free atoms on the surface as determined using a facetted surface model and the measured sputtering yield. © *2006 American Vacuum Society.*
[DOI: 10.1116/1.2212436]

I. INTRODUCTION

It is well established that the sputter erosion rate of a polycrystalline solid depends upon both the crystallographic orientation of the solid and the incoming ion trajectory. This effect is easily observed by viewing a sputtered polycrystalline target at low magnification or with the unaided eye. The etched pattern of grain relief is due to the variation in sputtering yield with grain orientation. Stark and Wendt reported this effect in 1912 for bismuth under hydrogen ion bombardment.[1]

Wehner and his co-workers conducted a more comprehensive study of the crystallographic nature of sputtering and found that sputtered atoms are ejected along close packed directions so that spot patterns are observed in the deposited films when single crystals are sputtered.[2] Measurement of the sputtering emission in tantalum by Anderson[3] demonstrated that atom ejection is predominately along the ⟨111⟩ close packed direction, but also to a lesser extent along ⟨001⟩ directions. More recently, Wickersham, Jr. and Zhang[4] reported on the relative strength of sputtered tantalum atom emission along the ⟨111⟩ and ⟨001⟩ directions for tantalum under magnetron sputtering conditions.

There are only a small number of publications on the variation of tantalum sputtering yield with grain orientation. Michaluk[5] suggested that the variation in tantalum sputter rate was more sensitive to changes in grain size than to changes in texture. However, neither details of the relative deposition rates nor target impedance data are provided which could also explain shifts in sputter rate. Tortorelli and Altstetter[6] measured the differential sputtering rates for grains of bcc niobium under 15 keV argon ion bombardment. They found that the sputtering yields of the niobium grains oriented with (111) planes perpendicular to the incoming 15 keV argon ion beam were about three times lower than the values expected for a random or amorphous Nb solid. They found good agreement between their measurements and the predictions from Silsbee[7] focus collision chains and channeling. As the ion energy is reduced, the Silsbee focus collision chain effect is expected to decrease. Calculations of the nonchanneled fraction for tantalum under 400 eV argon ion bombardment indicate that no differential grain sputtering should be detected due to channeling. This presents a conundrum in that grain relief occurs in magnetron sputtering of tantalum at energies below those in which channeling effects occur. What then is the source of the differential sputtering in magnetron sputtered tantalum grains?

Measurements of the relative sputtering yields of tantalum grains are provided in this article. The result shows that the sputtering yield of grains increases as the grain orientation changes from (111) to (100) to (110). Grains with their (110) planes parallel to the sputter surface erode at the highest rate. Grains with orientations near (111) erode with the slowest rate. The channeling model does not predict this behavior since at these low bombarding energies the ion is not expected to penetrate much beyond the first few atomic layers (~0.6 nm at 400 eV). Channeling calculations for tantalum show that at the low ion energies found during magnetron sputtering only a small fraction of the incoming argon ions are channeled. This occurs only when the grain orientation is with the (111) grain parallel to the sputter surface. No difference in sputtering yield is expected from channeling for argon ions impinging upon (001) or (011) tantalum surfaces at 400 eV.

II. EXPERIMENTAL PROCEDURE

Measurement of the relative sputter erosion rates of tantalum grains under magnetron sputtering conditions was accomplished by first cutting 25 mm diameter disks from electron beam melted ingot slices of 99.999% pure tantalum with an average grain size of around 3 cm. By using this large grain cast ingot material, it is a relatively simple task to make tantalum sputtering targets with only one to ten grains. Each 25 mm diameter tantalum sputtering target was cut from the ingot slice using electron discharge machining. The target was sputtered in a 25 mm diameter magnetron sputtering cathode with indirect water cooling. After sputtering the depth of erosion for each grain and the grain orientation were measured. A photograph of a typical tantalum target with

a)Electronic mail: cwickersham@ameritech.net

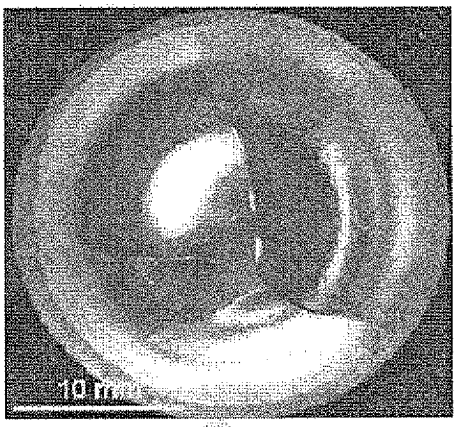

FIG. 1. Photograph of tantalum sputtering target with four grains after sputtering for 1 h at 100 W.

four grains is provided in Fig. 1. The weights of each tantalum target disk before and after sputtering were also measured.

The sputtering conditions were argon gas pressure of 2.7 Pa and target bias voltage ranging from around 500 V at the beginning of sputtering to around 400 V after 1.5 h of sputtering so that a constant power of 100 W was maintained. Under these conditions the tantalum grain eroded between 250 and 675 μm depending upon the sputtering time and grain orientation. The depth of grain erosion was measured with a point micrometer capable of reading to ± 5 μm.

The crystallographic orientation of each grain was measured after sputtering using electron backscattering diffraction (EBSD). Each sputtered tantalum disk was placed in a scanning electron microscopy (SEM) and each grain in the sputter erosion track was scanned in a 400×400 μm^2 square area using a 20 μm step to obtain 400 EBSD orientation measurements. The width of the erosion track was such that with these conditions, the data were collected from a relatively flat section at the bottom of the erosion track. Repeat measurements of the same sample gave the same Euler angles reproducible to within $\pm 3°$.

The sputtering yield for each grain, S_g, in units of at./ion was calculated from the measured erosion depth h_g using the relation

$$S_g = 1.6 \times 10^{-19} h_g A_{\text{eff}} \rho / A_v E_i / PT \text{MW}_{\text{Ta}}, \quad (1)$$

where ρ is the density of tantalum (16.684 g/cm^3), A_v is Avogadro's number, E_i is the average argon ion energy which in this case is taken to be 400 eV, P is the applied sputtering power in watts, T is the sputtering time in seconds, and MW_{Ta} is the tantalum molecular weight. A_{eff} is the effective sputtering area of the erosion track which is obtained from

$$A_{\text{eff}} = (W_b - W_a)/(\langle h_g \rangle \rho),$$

where W_b and W_a are the weights of the tantalum sputtering target before and after sputtering, respectively, and $\langle h_g \rangle$ is the average value of the individual grain erosion depths for the target sample. The effective sputtering area was determined to be 2.1 ± 0.3 cm^2.

The angles between each grain pole projection and the pole projections for the high symmetry bcc tantalum (001), (011), (112), and (111) low index planes were measured using a Wulff net. For these measurements, the Wulff net was scaled to match the EBSD inverse pole figure generated by the EBSD analysis software. The angles between the grain pole projection and the low index planes are accurate to within about 10%.

III. RESULTS

The Euler angles, the angles between the plane of each grain and the high symmetry planes for bcc tantalum [(011), (001), (112), and (111)], as well as the measured sputtering yield for each grain are provided in Table I. Figure 2 provides a graphical presentation of the data listed in Table I, using an inverse pole figure to represent the grain orientation and the gray scale value of each measurement in order to indicate the sputtering yield. The small number next to each spot is the ID number for the grain provided in Table I. While only 26 grains were measured, a clear trend can be seen in the data. Grains with plane orientations near the (111) plane had the lowest sputter erosion rate and grains with orientations near the (110) plane had the highest erosion rate. The sputtering yield increases by a factor of 2 as the grain plane normal to the incoming argon ion shifts from the (111) plane to the (011) plane.

The number of grains measured that are oriented near the (001) low index plane was not sufficient to make any strong conclusions about sputtering yield near the (001) plane. The selection of grain orientation is somewhat determined by the underlying texture of the cast ingot that tends to be around the (011)-(111) orientation.

IV. DISCUSSION

Using channeling calculations and the Silsbee focused collision cascade model of sputtering, a very small difference in sputter erosion rates is expected for tantalum under argon ion bombardment at low ion energies. Differences in the nonchanneled fraction of incident argon ions do not become significant until ion energies of over 600 eV are used. Table II provides the expected variation in sputtering yield due to channeling for bombardment along the ⟨001⟩, ⟨011⟩, and ⟨111⟩ directions. These calculations were made using the F_{nc} calculation method used by Tortorelli and Altstetter.[6] Based upon this analysis, the (111)-oriented grains are expected to have a sputtering yield that is only 4% less than the sputtering yield for (011)-oriented grains at 400 eV. The measured sputtering yield during magnetron sputtering of tantalum at 400–500 eV provided in this article indicates that the sputtering yield from (111) grains is lower than the sputtering yield from (110) grains by a factor of 2. A more accurate model of sputtering under magnetron conditions is obtained by considering the erosion and emission to be more controlled by the near surface structure of the tantalum target surface as proposed by Lehman and Sigmund.[8]

TABLE I. Experimental data for 26 tantalum grains showing sputtering yield and grain orientation (all angles in degrees).

			Euler angle			Angle				Erosion rate	Sputtering yield
ID	Sample	Grain	ϕ_1	Φ	ϕ_2	(011)	(001)	(112)	(111)	(nm/J)	(at./ion)
1	2498	1	198	14	35	33	14	20	38	0.69	0.52
2	2498	2	248	33	48	28	32	1.5	21	0.66	0.50
3	2498	3	135	50	44	32	48	14	4	0.68	0.51
4	2498	4	225	41	37	24	41	10	12	0.75	0.56
5	2498	5	311	49	39	28	48	14	6	0.60	0.45
6	2498	6	312	49	33	25	48	16	10	0.68	0.51
7	2499	1	229	9	8	35	9	22	46	1.04	0.77
8	2499	2	263	34	52	25	34	4	20	0.99	0.74
9	2499	3	197	41	77	8	41	21	26	1.10	0.82
10	2499	4	18	34	10	11	34	20	25	1.02	0.76
11	2499	5	244	39	34	24	39	8	16	0.75	0.56
12	2499	6	331	49	36	26	48	15	8	0.71	0.53
13	2499	7	329	49	36	26	48	16	7	0.73	0.54
14	2499	8	37	43	41	29	43	8	10	0.78	0.59
15	2795	1	29	42	30	21	42	12	15	0.79	0.59
16	2795	2	139	41	25	17	40	14	18	0.74	0.55
17	2795	3	146	42	16	11	42	19	23	0.77	0.58
18	2795	4	153	42	8	5	42	23	29	0.91	0.68
19	2796	1	214	41	34	21	40	10	13	0.84	0.63
20	2796	2	331	40	21	14	40	15	20	0.91	0.68
21	2796	3	335	42	14	10	42	21	24	0.91	0.68
22	2796	4	339	43	12	8	42	22	26	1.04	0.78
23	2800	1	134	33	31	22	33	8	19	1.16	0.87
24	2800	2	99	44	17	12	42	19	20	1.27	0.95
25	2801	1	40	33	35	24	33	6	20	0.64	0.47
26	2801	2	2	44	21	15	43	17	23	0.98	0.73

If surface sputtering is the predominate mode of sputtering for tantalum in magnetron systems, then the free atom surface density (FASD) can be a useful way to estimate the relative sputtering yield for various grain orientations. Figure 3 provides a series of schematic representations of the stacking arrangement of tantalum atoms for the four low index planes. The FASD is determined by counting the number of atoms per unit cell on the surface that are not blocked by another atom. For the case of the (011) close packed plane in tantalum shown in Fig. 3(a), the FASD is 12.8 at./nm^2. The tantalum (001) surface structure is shown in Fig. 3(b) and has a FASD value of 9.2 at./nm^2. Similarly, the FASD value for the tantalum (112) plane is 7.5 at./nm^2 [Fig. 3(c)]. The tantalum (111) plane has the lowest FASD for all the low index planes at 5.3 at./nm^2 [Fig. 3(d)]. This approach to determining the free atom surface density has been experimentally confirmed by Ermolov *et al.*[9] for tungsten using low energy ion scattering.

When the surface is not perfectly aligned with one of the low index planes, the surface under equilibrium conditions will consist of a series of the low index planes with steps. On average, the angle between the surface and the low index plane is created by periodically adding steps to the low index plane until the desired angle is created. This is illustrated in the (203) orientation example shown in Fig. 4. At the steps the atomic arrangement creates a situation where the atoms below the step are trapped beneath atoms in the upper sur-

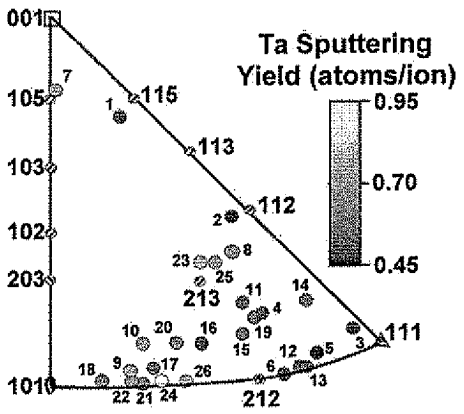

FIG. 2. Inverse pole figure showing relative tantalum sputtering rates for grains with different crystallographic orientations.

TABLE II. Calculations of F_{nc} (nonchanneled fraction) for argon ion bombardment of tantalum at normal incidence.

Ar Energy (eV)	F_{nc} ⟨001⟩	⟨011⟩	⟨111⟩
300	1	1	1
400	1	1	0.96
600	0.97	1	0.78
800	0.84	1	0.68
1000	0.75	1	0.61

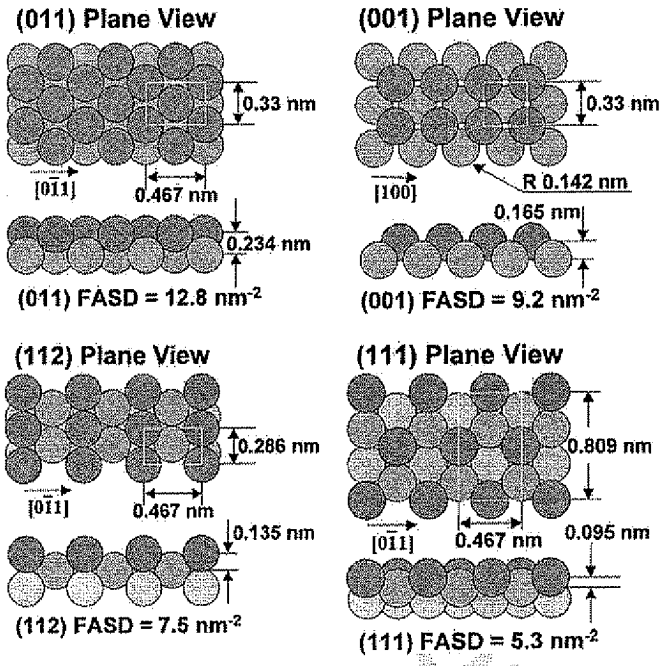

FIG. 3. Atomic surface structure models for determining the free atom surface density (FASD) of (a) the (011) plane of tantalum, (b) the (001) plane of tantalum, (c) the (112) plane of tantalum, and (d) the (111) plane of tantalum.

face and are unlikely to be sputtered by low energy ions. In this example the FASD decreases from 12.8 at./nm^2 for the (011) plane to 10.4 at./nm^2 for the (203) orientation. As the angle between the surface increases away from the low index plane, the FASD decreases. Figure 5 provides the FASD as a function of angle for surfaces around the four low index planes of tantalum.

The data in Fig. 5 are calculated assuming that the slope of the surface is such that the surface normal remains in a plane containing a low index [001] or [011] direction. This is a very simple surface rotation that makes calculating the FASD straightforward. However, there is no reason that the surfaces will follow this assumption. In fact, this is likely to be a rare event. The actual surfaces will tend to be a combination of slopes in at least two directions. This added complexity for the real surface results in slightly lower FASD than is provided in Fig. 5.

Table III provides a summary of the identification of each

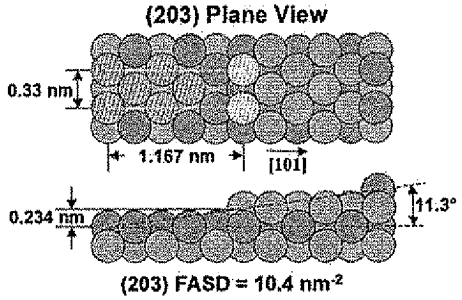

FIG. 4. Free atom surface density (FASD) for (203) plane of tantalum. Hatched atoms are the atoms in the unit cell that are included in the FASD.

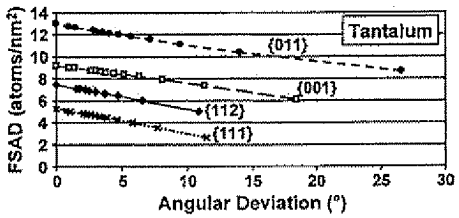

FIG. 5. Calculations of FASD for angular rotations from (011), (001), (112), and (111) planes.

grain, the measured sputtering yield for each grain, and the FASD determined for each grain as described above. The FASD values provided in Table III were obtained by determining which low index surface was nearest in angle to the measured grain orientation. Then the angular deviation between the low index plane and the plane of the grain parallel to the surface was used to determine the FASD value for that grain using the data in Fig. 5. These FASD values are listed in Table III and overestimate the FASD value by ignoring the complex rotation.

Figure 6 shows the correlation between the FASD as determined by the method described above for each grain and the measured sputtering yield for that grain. A linear least squares fit of these data provides a correlation coefficient of

TABLE III. Calculated free atom surface densities (FASDs) using the angle from the nearest low index plane.

ID	Sample	Grain	Sputtering yield (at./ion)	Nearest FASD (nm^{-2})
1	2498	1	0.52	6.9
2	2498	2	0.50	7.2
3	2498	3	0.51	4.4
4	2498	4	0.56	5.2
5	2498	5	0.45	3.9
6	2498	6	0.51	3.0
7	2499	1	0.77	7.7
8	2499	2	0.74	6.6
9	2499	3	0.82	11.5
10	2499	4	0.76	11.0
11	2499	5	0.56	5.7
12	2499	6	0.53	3.5
13	2499	7	0.54	3.6
14	2499	8	0.59	5.7
15	2795	1	0.59	4.7
16	2795	2	0.55	4.3
17	2795	3	0.58	11.0
18	2795	4	0.68	12.0
19	2796	1	0.63	5.2
20	2796	2	0.68	10.5
21	2796	3	0.68	11.2
22	2796	4	0.78	11.5
23	2800	1	0.87	5.7
24	2800	2	0.95	10.9
25	2801	1	0.47	6.1
26	2801	2	0.73	10.4

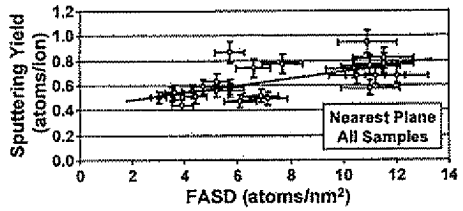

FIG. 6. Correlation between FASD for nearest low index plane and sputter yield.

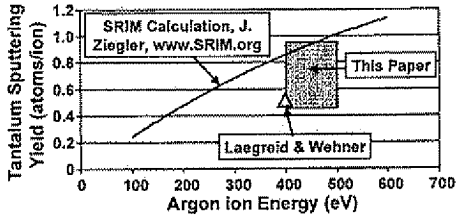

FIG. 8. Sputtering yield for tantalum under normal argon ion bombardment from SRIM calculations (solid line) and the results from Laegreid and Wehner (triangle) and the measurements in this article (square).

0.4. It is clear that there is a great deal of scatter in the data, but grains with orientations near (111) have a lower sputtering yield than grains near (011).

One of the sources of the scatter in the data in Fig. 6 is the consistency of the sputtering conditions from sample to sample. The sputtering conditions for each sample could not be maintained exactly consistent. Variation in sputtering burn-in time and variation in the sputtering voltage and current contribute to variation in the observed sputtering yield. One sample, 2499, had eight grains in the erosion track and with this sample the sputtering conditions are more identical from grain to grain. Figure 7 provides a graph of the correlation between the FASD for each grain in sample 2499 calculated as described above and the measured sputtering yield. A much stronger correlation is obtained from this sample with the correlation coefficient of 0.7.

The absolute value of the sputtering yield that we obtained is in good agreement with the measured values reported in the literature for tantalum (0.5 at./ion at 400 eV)[10] and calculated values for tantalum using SRIM (0.85 at./ion at 400 eV).[11] Figure 8 provides a graphical comparison of the measured sputtering yields from the literature, SRIM calculations, and current measured values.

In future work, preparation of samples with grain sizes of a few millimeters in diameter and a random crystallographic texture should provide a more accurate determination of the effect of grain orientation on sputtering yield. With a single sample, around 30 different grain orientations could be measured in this way. Creation of this sample by powder metallurgical techniques would be an advantage since this would provide a random crystallographic orientation with grain orientations near the (001) pole and center of the inverse pole figure. In addition, the experiments should be conducted under constant voltage conditions rather than constant power.

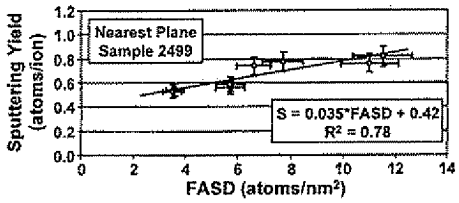

FIG. 7. Correlation between FASD for nearest low index plane and sputtering yield for sample 2499.

V. CONCLUSION

Measurements of the sputtering yield of tantalum grains under magnetron sputtering conditions have been made and the sputtering yields are found to increase by a factor of 2 as the grain orientation changes from (111) to (011) planes parallel to the sputtering surface. This difference in sputter yield is not expected from channeling considerations since the argon ion energies are not sufficient to cause a significant channeling effect. The difference in sputtering yield is attributed to the change in free atom surface density with grain orientation.

[1]J. Stark and G. Wendt, Ann. Phys. **38**, 941 (1912).
[2]G. K. Wehner, J. Appl. Phys. **26**, 1056 (1955).
[3]G. S. Anderson, J. Appl. Phys. **34**, 659 (1963).
[4]C. E. Wickersham Jr., and Z. Zhang, J. Electron. Mater. **34**, 1474 (2005).
[5]C. Michaluk, J. Electron. Mater. **31**, 2 (2002).
[6]P. F. Tortorelli and C. J. Altstetter, Radiat. Eff. **51**, 241 (1980).
[7]R. H. Silsbee, J. Appl. Phys. **28**, 1246 (1957).
[8]Chr. Lehmann and P. Sigmund, Phys. Status Solidi **16**, 507 (1966).
[9]S. N. Ermolov, V. G. Glebovskii, R. Cortenraad, B. Moest, E. D. Shitnov, A. V. Denier van der Gon, and H. H. Brongersma, Phys. Met. Metallogr. **93**, 443 (2002).
[10]N. Laegreid and G. K. Wehner, J. Appl. Phys. **32**, 365 (1961).
[11]J. Ziegler, SRIM, www.SRIM.org